Czech Technical University in Prague
Faculty of Nuclear Sciences and Physical Engineering

Department of Physics

Entanglement theory and manipulation of entangled photon pairs

Research project

Author: Elisabeth Andriantsarazo
Supervisor: Ing. Václav Potoček, Ph.D.
Academic year: 2017/2018

Prohlášení

Prohlašuji, že jsem svůj výzkumný úkol vypracovala samostatně a použila jsem pouze podklady (literaturu, projekty) uvedené v přiloženém seznamu.

Nemám závažný důvod proti použití tohoto školního díla ve smyslu § 60 Zákona č. 121/200 Sb., o právu autorském, o právech souvisejících s právem autorským a o změně některých zákonů (autorský zákon).

V Praze dne 31. 8. 2018

.....
Elisabeth Andriantsarazo

Acknowledgment

I would like to express my gratitude to my supervisor Ing. Václav Potoček, PhD. for his support and kind guidance not only in this research project but in all my projects. I would also like to thank all members of IQO group in Paderborn university for all their generous advices and support, especially to Dr. Vahid Ansari who supervised experiments during my stay and encouraged me. I am also very grateful and thankful to my amazing family for supporting me and helping me during my studies.

Elisabeth Andriantsarazo

Název:

Teorie provázání a manipulace s provázanými fotonovými páry

Autorka: Elisabeth Andriantsarazo

Druh práce: Výzkumný úkol

Vedoucí práce: Ing. Václav Potoček, Ph.D.
Department of Physics, Faculty of Nuclear Sciences and Physical Engineering, Czech Technical University in Prague

Abstrakt:

Zkoumání kvantové optiky teprve před nedávnem přešlo z roviny teoretické do roviny praktické především díky dostupnosti laserových technologií a nelineárních optických elementů. Fotony jsou zároveň nejpraktičtější a nejjednodušší způsob jak v laboratoři simulovat kvantové bity a jak zkoumat jejich provázanost. Do budoucna se s kvantovou optikou počítá především v komunikačních a bezpečnostních protokolech. V této práci zkoumáme metody provázání a generaci jednotlivých fotonů pomocí krystalů a jevu spontánní parametrické konverze. Předkládáme několik experimentálních aparatur a teoretický úvod do jednotlivých oborů zkoumání, které s vývojem těchto aparatur souvisí. Těmi jsou především nelineární a krystalová optika, popis průchodu paprsku používanými optickými elementy, kvantování elektromagnetického pole a teorie kvantového provázání. Následně je ukázána radikální změna v naměřených výsledcích při přechodu od klasického světla k velmi slabým intenzitám, respektive při přechodu od klasické optiky ke kvantové optice a jednotlivým fotonům.

Klíčová slova: Nelineární optika, krystalová optika, PDC, provázané fotony

Title:

Entanglement theory and manipulation of entangled photon pairs

Author: Elisabeth Andriantsarazo

Supervisor: Ing. Václav Potoček, Ph.D.
Department of Physics, Faculty of Nuclear Sciences and Physical Engineering, Czech Technical University in Prague

Abstract:

Research in quantum optics only recently passed from theoretical plane to the practical level, mainly due to the availability of laser technologies and non-linear optical elements. Photons are also a practical and simple way to simulate quantum bits and study entanglement in the laboratory. In the future, quantum optics is expected to be mainly used in communications and security protocols. In this work we investigate methods of single-photon and entangled photon generation using crystals and the phenomenon of spontaneous parametric downconversion. We present several experimental apparatures and a theoretical introduction to the various fields of research that are related to their development. These are primarily nonlinear and crystal optics, a description of the beam passage through optical elements, quantization of the electromagnetic field, and the theory of quantum entanglement. Furthemore, a radical change in the measured results is shown in the transition from classical light to very weak field intensities, a.k.a. in the transition from classical optics to quantum optics and single-photons.

Key words: Non-linear optics, crystal optics, PDC, entangled photons

Contents

List of Figures

Introduction

This work focuses on a brief theoretical summary of non-linear, crystal and quantum optics. In other words, it should contain the background necessary for understanding processes behind single-photon and entangled photon pair generation. We provide two possible approaches how to understand light, which is the classical one (where we describe light as a wave or a beam) and the quantum one (where we use the idea of photons, quanta of electromagnetic field). We experimentally show that we in fact need to quantize the field in order to get correct predictions for what we see in reality. Fast development of reliable single-photon sources is vital for correct operation of communication and security protocols, designed in theory. These protocols should allow us to securely transfer and secure our data much more efficiently than today and most of them need fast working single-photon source. In this work we also provide two possible ways of creating single-photons which is either by a bulk or a wave-guided source. Both of them have their pros and cons and we provide thorough description of both media, together with explanation of their differences.

We also focus on building experimental set-ups necessary for detecting single-photons and provide a description of all parts and optical elements used, including detectors. We also add summary of the theory behind single-photon detection and coincidence counting. In order to build a functioning apparatus for data encryption and communication we need to figure out what detection processes fit our needs the best.

At the end of this work we show a proof that we actually created single-photons. We provide an explanation of what we plan to do next and how we want to further increase efficiency of all the vital parts of our apparatus.

Chapter 1

Non-linear and crystal optics

In this chapter we will discuss theory of non-linear processes in crystals, that are essential to single-photon generation in both our experiments introduced in sections 7.1 and 7.2. The main sources of information for this chapter were [1] and [2].

1.1 Non-linear optics

After first working laser was introduced, many new optical phenomena were observed, mainly non-linear optical processes. We can describe them as: "*...phenomena that occur as a consequence of the modification of the optical properties of a material system by the presence of light... they occur when the response of a material system to an applied optical field depends in a non-linear manner on the strength of the optical field.*", [1].
Let us consider a dielectric material. It can be described as a collection of electric dipoles and we can present a new term called macroscopic polarization, $\tilde{P}(t)$. The non-linearity is then described by the dipole moment per unit volume in such medium and the polarization vector $\tilde{P}(t)$ then depends on the strength of the optical field that is applied, $\tilde{E}(t)$. In linear optics we write:

$$\tilde{P}(t) = \varepsilon_0 \chi^{(1)} \tilde{E}(t), \tag{1.1}$$

where $\chi^{(1)}$ is the linear susceptibility and ε_0 is the permittivity. In non-linear optics, however, equation (1.1) has to be generalized:

$$\tilde{P}(t) = \varepsilon_0 \left[\chi^{(1)} \tilde{E}(t) + \chi^{(2)} \tilde{E}^2(t) + \chi^{(3)} \tilde{E}^3(t) + ... \right], \tag{1.2}$$

where $\tilde{P}^{(i)}$ are known as the i-th order non-linear optical susceptibilities. We will refer to the $\tilde{P}^{(2)}(t) = \varepsilon_0 \chi^{(2)} \tilde{E}^2(t)$ as the second-order non-linear polarization and $\tilde{P}^{(3)}(t) = \varepsilon_0 \chi^{(3)} \tilde{E}^3(t)$ as the third-order non-linear polarization. Higher orders are unnecessary as for now because they are too small. [1]

[1] Equation (1.2) becomes invalid once the laser field strength is comparable to the characteristic atomic field strength E_{at}:

$$E_{at} = \frac{e}{4\pi\varepsilon_0 a_0^2}, \tag{1.3}$$

where e is the charge of electron and $a_0 = 4\pi\varepsilon_0\hbar^2/me^2$ is the Bohr atom radius. That is because the power series expansion does not converge once ionization of the matter occur. Laser intensity at peak

Time varying polarization $\tilde{P}(t)$ of a medium acts as a source of new components of the electromagnetic field. If we want to explore this phenomena and how a light beam propagates through non-linear materials we shall start with Maxwell's equations:

$$\nabla \times \vec{E} = -\frac{\partial \vec{B}}{\partial t} \tag{1.4}$$

$$\nabla \times \vec{H} = \frac{\partial \vec{D}}{\partial t} \tag{1.5}$$

$$\nabla \vec{D} = 0 \tag{1.6}$$

$$\nabla \vec{B} = 0, \tag{1.7}$$

where $\vec{D} = \varepsilon_0 \vec{E} + \vec{P}$ and $\vec{H} = \vec{B}/\mu_0$. From (1.4), (1.5), (1.6) and (1.7) an optical wave equation can be derived:

$$\nabla^2 \vec{E} - \frac{1}{c^2}\frac{\partial^2 \vec{E}}{\partial t^2} = \frac{1}{\varepsilon_0 c^2}\frac{\partial^2 \vec{P}}{\partial t^2}, \tag{1.8}$$

where c is the speed of light in vacuum. We now split $\vec{P}$ into linear and non-linear parts:

$$\vec{P} = \vec{P}^{(1)} + \vec{P}^{NL}, \tag{1.9}$$

and we get a wave equation for case of an isotropic, dispersionless material:

$$\nabla^2 \vec{E} - \frac{\varepsilon}{c^2}\frac{\partial^2 \vec{E}}{\partial t^2} = \frac{1}{\varepsilon_0 c^2}\frac{\partial^2 \vec{P}^{NL}}{\partial t^2}, \tag{1.10}$$

where ε is the relative permittivity. Here we can see that the non-linear response of a material acts as a source term and is responsible for phenomena we observe.

1.2 Crystal optics

One of the main things one needs to focus on when studying crystal optics is symmetry of a crystalline medium. The crystal can either be **centrosymmetric** or **non-centrosymmetric**, meaning it either posses inversion symmetry or it doesn't. Crystals can also be divided in optically **isotropic** or **anisotropic**, meaning it doesn't exhibit birefringence[2] or it does. Most used crystals in non-linear optics are non-centrosymmetric and optically anisotropic, but whether the material exhibits birefringence or not has no link to its centrosymmetry. Both crystals used in our experiment, BBO (beta-barium borate) and KTP (potassium titanyl phosphate), are indeed anisotropic and birefringent. In the next section we shall briefly cover light propagation in anisotropic media. How birefringence originates is described in section 2.3.

field strength is approximately $I_{max} = 3,5 \times 10^{16}\mathrm{W/cm}^2$. We can see there is no need for us to worry about these effects as we work with laser intensities in terms of watts.

[2]Birefringence, also known as double refraction, is an optical property of a medium that has a refractive index dependent on polarization plane and propagation direction of incoming light. For more see section 2.3.

1.2.1 Light propagation in anisotropic media

First we need to determine the direction of vectors $\vec{E}, \vec{D}, \vec{B}$ and $\vec{H}$ appearing in Maxwell's equations as the direction in which the light emerging from our crystalline media is polarized depends on those vectors. For non-magnetic medium with no free charges Maxwell's equations read:

$$\nabla \vec{D} = 0 \tag{1.11}$$

$$\nabla \vec{B} = 0 \tag{1.12}$$

$$\nabla \times \vec{E} = -\frac{\partial \vec{B}}{\partial t} \tag{1.13}$$

$$\nabla \times \vec{B} = -\frac{\partial \vec{D}}{\partial t}. \tag{1.14}$$

Further simplifications can be made, such as only considering plane EM waves with wave vector $\vec{k}$ only depending on z-direction. This reduces equation (1.13) to $\partial B_z/\partial t = 0$ which makes $\vec{B} = (0, 0, B_z)$ and also $\vec{H} = (0, 0, H_z)$. Same conclusion can be made about $\vec{D}$. By choosing the y axis to lie along $\vec{B}$ it follows from equation (1.14) that $\vec{D}$ lies along the x axis. And lastly we get from equation (1.13) that $E_y = 0$. Representation of all our conclusions can be seen in figure 1.1. The plane of polarization of the propagating light

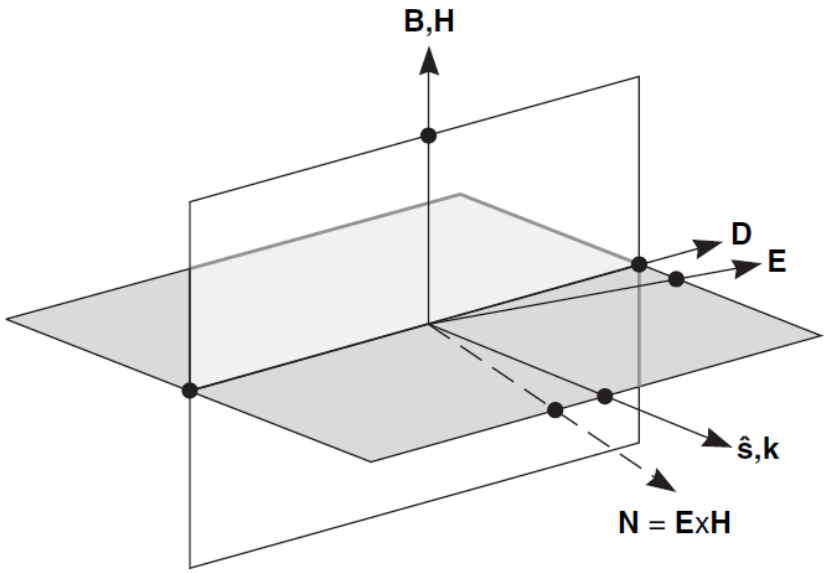

Figure 1.1: Directions of vector fields in non-magnetic medium with no free charges. $\vec{B}, \vec{H}$ and $\vec{D}$ lie in the same plane with $\vec{D}$ being perpendicular to the two. $\vec{E}$ is coplanar with $\vec{D}$. Source: [2].

is now defined as the plane perpendicular to $\vec{B}$. We need one more condition to be able to determine $\vec{E}$ and that is the constitutive relation:

$$\vec{D} = \varepsilon_0 \varepsilon \vec{E}, \tag{1.15}$$

where in anisotropic media ε becomes a tensor called dielectric constant tensor. The reason for that is because $\vec{D}$ and $\vec{E}$ are not always parallel in anisotropic media. Hence we need

a tensor to define the exact relation between them:

$$\begin{pmatrix} D_x \\ D_y \\ D_z \end{pmatrix} = \varepsilon_0 \begin{pmatrix} \varepsilon_{xx} & 0 & 0 \\ 0 & \varepsilon_{yy} & 0 \\ 0 & 0 & \varepsilon_{zz} \end{pmatrix} \begin{pmatrix} E_x \\ E_y \\ E_z \end{pmatrix} \tag{1.16}$$

where $\varepsilon_{ii}, i \in \{x, y, z\}$ are called principal dielectric constants. Media with all three dielectric constants different are called **biaxial**, those with two same and one different are called **uniaxial** and for all three the same we get **isotropic medium**. Maxwell's equations and constitutive relation are satisfied for arbitrary $\vec{k}$ only for two directions of $\vec{D}$ mutually orthogonal. They define the plane of polarization of the only two wave solutions allowed. The dielectric constants and refractive indices of a crystal are connected through following equation:

$$\frac{x^2}{\varepsilon_{xx}} + \frac{y^2}{\varepsilon_{yy}} + \frac{z^2}{\varepsilon_{zz}} = \frac{x^2}{n_x} + \frac{y^2}{n_y} + \frac{z^2}{n_z} = 1, \tag{1.17}$$

where x, y, z is a special set of orthogonal axis called principal dielectric axes. In general all three refractive indices are different from each other, but we shall simplify things and focus on uniaxial case, where $n_x = n_y$. We define:

$$n_x \equiv n_o, \quad n_z \equiv n_e, \tag{1.18}$$

where the subscript o, e corresponds to ordinary and extraordinary refractive index respectively. The z axis is called the optic axis. One more thing should be emphasized and that is the fact that second-order non-linear effects can only happen in non-centrosymmetric crystals as the $\chi^{(2)}$ part of equations vanishes in media with inversion symmetry. For this reason we mainly focus on non-centrosymmetric crystalline media.

1.3 Non-linear optics in crystals

We shall now explore non-linear coefficients (mainly susceptibility) as they are most important in non-linear processes in crystals. First thing that we need to bear in mind is that the equation (1.2) changes if we consider the field frequency dependency. A complete description lies within the polarization vector that is now given by:

$$P_i(\omega) = \varepsilon_0 \sum_{jk} \sum_{nm} \chi^{(2)}_{ijk}(\omega_m + \omega_n, \omega_m, \omega_n) E_j(\omega_n) E_k(\omega_m), \tag{1.19}$$

where $i, j, k \in \{x, y, z\}$. We only work with three different frequencies, since the non-linear process behind entangled photon generation requires only three-field interaction. The susceptibility, hiding all the details of media characteristics, now becomes a tensor. The overall number of tensors present in equation (1.19) is six:

$$\chi^{(2)}_{ijk}(\omega_1, -\omega_2, \omega_3), \quad \chi^{(2)}_{ijk}(\omega_1, \omega_3, -\omega_2), \quad \chi^{(2)}_{ijk}(\omega_2, \omega_3, -\omega_1) \tag{1.20}$$

$$\chi^{(2)}_{ijk}(\omega_2, -\omega_1, \omega_3), \quad \chi^{(2)}_{ijk}(\omega_3, \omega_1, \omega_2), \quad \chi^{(2)}_{ijk}(\omega_3, \omega_2, \omega_1). \tag{1.21}$$

We need to count six more for switching each frequency with its negative counterpart. These 12 tensors consist of 27 Cartesian components which means we would need to calculate 324 different complex number in order to properly describe our interaction. Fortunately, there are symmetry properties of the non-linear susceptibility that helps us determine all the constants necessary. First, we can interchange n with m and j with k, such that:

$$\chi^{(2)}_{ijk}(\omega_m + \omega_n, \omega_m, \omega_n) = \chi^{(2)}_{ikj}(\omega_m + \omega_n, \omega_n, \omega_m). \tag{1.22}$$

This property, known as intrinsic permutation symmetry, physically means that it doesn't matter which field is the first and which is the second. Additional symmetries emerge once we assume lossless media. Then all the components of susceptibility tensor become real and all of the arguments can be interchanged:

$$\chi^{(2)}_{ijk}(\omega_3 = \omega_1 + \omega_2) = \chi^{(2)}_{jki}(-\omega_1 = \omega_2 - \omega_3). \tag{1.23}$$

We also needed to interchange corresponding Cartesian indices while inverting the sign of the frequencies. After applying all these conditions we come to a conclusion that only 27 real numbers must be determined. There are even more symmetries, used to further simplify our calculations, that can lower the number of independent elements down to 10 or even further.

Chapter 2

Light propagation through optical devices

In this section we shall briefly cover light in bulk matter, or rather transparent dielectrics. The theory of light propagation and transmission through such media was mainly acquired from [3], [4] and [5]. Optical devices used in our experimental set-ups (see sections 7.1 and 7.2) and their influence on a light beam is described as a response of dielectric materials on incident electromagnetic field. Function of such optical device is to reshape a portion of an incident wavefront[1] and create an image. For simplicity we shall further ignore any diffraction effects, but in reality various polishes are being used on each surface in order to keep a beam loss, absorption and scattering as low as possible.

2.1 Plane mirrors

Planar surfaces have a simple role compared to other optical devices. Their role is to guide a laser beam to a desired place under some degree of rotation. If a mirror is rotated under θ the beam rotates under 2θ. Mirrors have different surfaces used for various needs. If a surface is smooth, we talk about **specular reflection**, if a surface is rough, we talk about **diffuse reflection**. In our case we only use smooth surfaces, as rough ones lead to rays being reflected in various directions. An important characteristic of a plane mirror is its reflectivity which is generally a function of incident beam wavelength. The rest of the light beam is then usually absorbed by the mirror, scattered elsewhere or transmitted. The ratio of reflected to transmitted light by a smooth surface is given by Fresnel equations. Consider incident monochromatic wave given by:

$$\vec{E}_i = \vec{E}_{0i} \cos(\vec{k}_i \vec{r} - \omega_i t), \tag{2.1}$$

where the amplitude vector $\vec{E}_{0i}$ is constant in time. Reflected and transmitted waves are then given by:

$$\vec{E}_r = \vec{E}_{0r} \cos(\vec{k}_r \vec{r} - \omega_r t) \tag{2.2}$$

$$\vec{E}_t = \vec{E}_{0t} \cos(\vec{k}_t \vec{r} - \omega_t t). \tag{2.3}$$

[1] Wavefront for electromagnetic waves is defined as a set of points with identical position propagation and identical phase. For a collimated light such wavefront is a plane wave.

Encountering a surface with different refractive index can change the overall polarization plane of the incident beam. We define the primary polarization of the beam as either S-polarized (where electric field is normal to the plane of incidence) or P-polarized (where electric field is in the plane of incidence). The amount of reflected and transmitted light differs for the two different incident polarization planes. For the perpendicular case we get the reflection r and transmission t index as:

$$r \equiv \frac{E_{0r}}{E_{0i}} = \frac{n_i \cos\theta_i - n_t \cos\theta_t}{n_i \cos\theta_i + n_t \cos\theta_t} \tag{2.4}$$

$$t \equiv \frac{E_{0t}}{E_{0i}} = \frac{2n_i \cos\theta_i}{n_i \cos\theta_i + n_t \cos\theta_t}. \tag{2.5}$$

For the parallel case we get following coefficients:

$$r_{||} = \frac{n_t \cos\theta_i - n_i \cos\theta_t}{n_i \cos\theta_t + n_t \cos\theta_i} \tag{2.6}$$

$$t_{||} = \frac{2n_i \cos\theta_i}{n_i \cos\theta_t + n_t \cos\theta_i}. \tag{2.7}$$

2.2 Lenses

Lens can be defined as *"...a refracting device that reconfigures transmitted energy distribution."* [[3]]. Their role in an optical configuration is to collect beam waves and transform one wavefront into another. All lens shapes discussed in this section will be conic sections. Convex lenses keep a beam from diverging. They converge (focus) the beam to a point in space, whereas concave lens causes parallel rays to diverge. Such refraction happens according to well known Snell's law:

$$n_1 \sin\varphi_1 = n_2 \sin\varphi_2, \tag{2.8}$$

where different indices correspond to different media. The refraction index n_i in this case corresponds to the absolute index of refraction defined as:

$$n \equiv \frac{c}{v} = \sqrt{\frac{\varepsilon\mu}{\varepsilon_0\mu_0}}, \tag{2.9}$$

where v is the phase speed in respective medium. Both angles φ_i in equation (2.8) are measured from the normal of the boundary. A refraction equation of a lens is given as follows:

$$\frac{n_1}{s} + \frac{n_2}{s'} = \frac{n_2 - n_1}{R}, \tag{2.10}$$

where s is the object distance, s' is the image distance and R is the radius of our spherical interface. A focal length f of our lens is then given by:

$$\frac{1}{s} + \frac{1}{s'} = \frac{1}{f}, \tag{2.11}$$

which can be used to distinguish between converging and diverging lenses as we can see in figure 2.1. All the equations above are just an approximation used for a case of thin

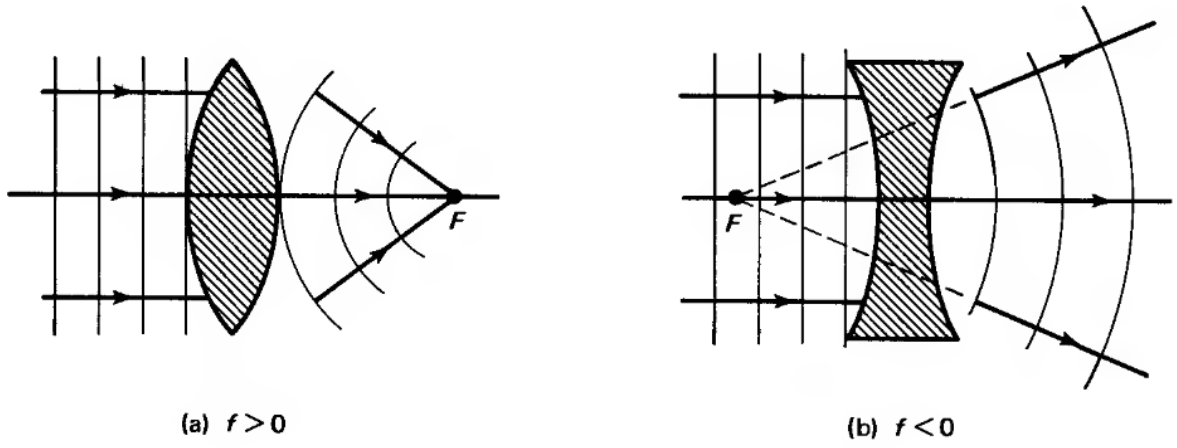

Figure 2.1: Different types of lenses based on different focal lenght. For positive focal length we get a convex lens and for negative focal length we get a concave lens. Source [4].

lenses. In this case thickness of a lens can be neglected compared to R. For complex optical system description we can no longer neglect effects due to thickness of a lens, which leads us to refraction and reflection being both described by 2x2 matrices. This approach is convenient for describing a beam going through mixture of multiple different lenses in a optical set-up. If we were to predict values for the height and slope angle of any ray traversing a thick lens, we would need to determine a compound matrix called the system matrix. Such matrix consists of different matrices for translation, refraction and reflection of the ray. The translation matrix is given by:

$$\begin{pmatrix} 1 & L \\ 0 & 1 \end{pmatrix} \tag{2.12}$$

where L is axial progress of the ray in homogeneous medium. The refraction matrix is given as follows:

$$\begin{pmatrix} 1 & 0 \\ \frac{1}{R}\left(\frac{n_1}{n_2} - 1\right) & \frac{n_1}{n_2} \end{pmatrix} \tag{2.13}$$

and the reflection matrix, which can also be used for a spherical mirror, is given by:

$$\begin{pmatrix} 1 & 0 \\ \frac{2}{R} & 1 \end{pmatrix}. \tag{2.14}$$

For $R > 0$ we get a convex lens, for $R < 0$ we get a concave lens. Now, if we were to describe a thick lens of thickness t with refraction index n_L using these matrices, we would multiply a refraction matrix with a translation matrix with a refraction matrix again, which would give us our overall system matrix:

$$\mathbb{M}_{thick} = \begin{pmatrix} 1 & 0 \\ \frac{n_L - n_2}{n_2 R_2} & \frac{n_L}{n_2} \end{pmatrix} \begin{pmatrix} 1 & t \\ 0 & 1 \end{pmatrix} \begin{pmatrix} 1 & 0 \\ \frac{n_1 - n_L}{n_L R_1} & \frac{n_1}{n_L} \end{pmatrix}, \tag{2.15}$$

where R_1 describes curvature of the front part of our lens and R_2 describes curvature of the back part. For a lens surrounded by the same medium $n_1 = n_2$ we get:

$$\begin{pmatrix} 1 & 0 \\ \frac{n_L - n}{n}\left(\frac{1}{R_2} - \frac{1}{R_1}\right) & 1 \end{pmatrix}. \tag{2.16}$$

From the matrix element M_{21} we get a new equation for focal length:

$$M_{21} = \frac{n_L - n}{n}\left(\frac{1}{R_2} - \frac{1}{R_1}\right) = -\frac{1}{f}. \tag{2.17}$$

Determinant of the overall system matrix can be calculated as:

$$\det \mathbb{M}_{thick} = \frac{n_i}{n_f}, \tag{2.18}$$

where index i stands for initial medium and f stands for final medium of our optical set-up. As we can see this approach gives us a quick way of determining the beam propagation. Nowadays these calculations can be made by several simple computer programs.

2.3 Production of polarized light

Light can be treated as a transverse electromagnetic wave, meaning it consists of oscillations occurring perpendicular to the direction of energy transfer. In case of **linearly polarized light** the plane of polarization is the plane of electric field $\vec{E}$ orientation which is constant with sign varying in time. The same plane also contains $\vec{k}$, the propagation vector. Overall field can be described as sum of two perpendicular waves:

$$\vec{E}(z,t) = \vec{E}_x(z,t) + \vec{E}_y(z,t), \tag{2.19}$$

where $\vec{E}_x(z,t) = \hat{\vec{x}} E_{0x}\cos(kz - \omega t)$ and $\vec{E}_y(z,t) = \hat{\vec{y}} E_{0y}\cos(kz - \omega t + \varepsilon)$, ε being the relative phase difference between both waves, $\hat{\vec{x}}$ and $\hat{\vec{y}}$ representing Cartesian axes. If both waves have equal amplitudes, $E_{0x} = E_{0y} = E_0$, and their phase difference $\varepsilon = -\pi/2 + 2\pi n\, n \in \mathbb{Z}$ we talk about **circular polarization**. Such wave can be described as follows:

$$\vec{E} = E_0(\hat{\vec{x}}\cos(kz - \omega t) + \hat{\vec{y}}\sin(kz - \omega t). \tag{2.20}$$

Polarized light can be produced by **absorption**, **reflection**, **scattering** or **birefringence**. The ability to further modify previously polarized light is called optical activity. The most important cases for our research are the first and the last, but we shall briefly go through all the cases listed here.

In case of absorption we shall cover mainly dichroic polarisers as they are frequently used in laboratory. Their role is to selectively absorb some directions of $\vec{E}$ and transmit the rest along a transmission axis, unique for the material. We must just bear in mind that every dichroic material has its dependency on wavelength, so we must choose the right one when using it in an experiment.

As for the second case, polarization is achieved by reflection from dielectric surfaces. Such light is only partially polarized as the preferred direction of $\vec{E}$ is preserved and the other

is reduced in brightness. This phenomenon occurs in our experiments mostly unintentionally, but the overall effect is rather insignificant. For these reasons we neglect polarization produced by reflection in all our measurements.
In the third care we shall start with explanation of the scattering phenomenon itself. Scattering of light signifies the removal of energy from an incident wave by a medium that consists of elementary scattering units. Such systems can be understood as an electric charge bound to an atom nucleus that is set into forced oscillation by the incident light. Response depends on frequency ω of incoming light and the resonant frequency ω_0 of the scattering unit, which mostly lies in the ultraviolet region. For these reasons we suppose $\omega << \omega_0$ which means that induced oscillation are independent of the incident light frequency. Polarization by scattering is usually used in non-linear optics where the incident light scatters from an active media and is further modified by the resonant frequencies of the medium.
Lastly we have the birefringence, producing two refracted beams. The two different refraction indices of the material correspond to different vibrations of the incident electric field $\vec{E}$; n_x for E_x and n_y for E_y which in addition differ for optical frequencies. In fact all important physical properties of a birefringent crystal is frequency dependent, for example the extinction coefficient k or the refractive index n itself. Together they define the complex refractive index:

$$\tilde{n} = n + ik. \tag{2.21}$$

For an ideal birefringent material $k_x = k_y$ and $n_x \neq n_y$. We shall define the two different directions as ordinary and extraordinary, see equation (1.18). Both beams emerging from the crystal are linearly polarized and the two polarization planes are orthogonal. The length difference for the ordinary and extraordinary path gives an overall phase shift for one of the beam. This shift can be calculated as follows. First we define the difference in optical path:

$$\Delta = |n_e - n_o|d, \tag{2.22}$$

where d is the crystal thickness. The phase shift, or phase difference, is then given by:

$$\Delta\varphi = 2\pi\frac{\Delta}{\lambda_0} = \frac{2\pi}{\lambda_0}|n_e - n_o|d, \tag{2.23}$$

where λ_0 is called the vacuum wavelength. For $\Delta\varphi = \pi$ we have a half-wave plate, for $\Delta\varphi = \frac{\pi}{2}$ we have a quarter-wave plate.

Chapter 3

Quantization of electromagnetic field

In this chapter field quantization is presented, mainly for the single-mode case. That is because in our experiments (see section 7.2) we use a single-photon source producing single-mode field. One section is dedicated to multi-mode case and difference between the two. In previous sections we explored ways of light propagation as waves and beams in non-linear and crystalline media and in several optical elements. Such approach has of course its limitations, since it is a classical one. If we were to really understand the way single photons behave, we would need to switch to quantum physics. In this chapter we present how such transition is done. Theory behind this introduction was mainly acquired from [6] and [7].

3.1 Quantization of a single-mode field

A way to quantize the electromagnetic field is to make an analogy between photon and a simple-harmonic oscillator. Let's have a radiation field confined in one-dimensional cavity of length L along the z-axis. Let's also assume the cavity has perfectly conducting walls at $z = 0$ and $z = L$. We start with Maxwell equations without sources:

$$\nabla \times \vec{E} = \frac{\partial \vec{B}}{\partial t} \tag{3.1}$$

$$\nabla \times \vec{B} = \mu_0 \varepsilon_0 \frac{\partial \vec{E}}{\partial t} \tag{3.2}$$

$$\nabla \vec{B} = 0 \tag{3.3}$$

$$\nabla \vec{E} = 0. \tag{3.4}$$

A solution that satisfies such conditions is for example given by:

$$E_x(z,t) = \sqrt{\frac{2\omega^2}{V\varepsilon_0}} q(t) \sin(kz), \tag{3.5}$$

where ω is the field frequency, $k = \omega/c$, V is the effective volume of our cavity and $q(t)$ is canonical position. Magnetic field is given by:

$$B_y(z,t) = \frac{\mu_0 \varepsilon_0}{k} \sqrt{\frac{2\omega^2}{V\varepsilon_0}} \dot{q}(t) \cos(kz), \tag{3.6}$$

where $\dot{q}(t) = p(t)$.
The Hamiltonian of the single mode is given by:

$$H = \frac{1}{2}\int \left[\varepsilon_0 E_x^2(z,t) + \frac{1}{\mu_0} B_y^2(z,t)\right] \mathrm{dV}, \tag{3.7}$$

which gives us:

$$H = \frac{1}{2}(p^2 + \omega^2 q^2). \tag{3.8}$$

Using correspondence rule, $q \to \hat{q}$; $p \to \hat{p}$ where both $\hat{q}$ and $\hat{p}$ are Hermitian operators and they satisfy the commutation relation $[\hat{q}, \hat{p}] = i\hbar$, we get:

$$\hat{E}_x(z,t) = \sqrt{\frac{2\omega^2}{V\varepsilon_0}}\hat{q}(t)\sin(kz) \tag{3.9}$$

$$\hat{B}_y(z,t) = \frac{\mu_0\varepsilon_0}{k}\sqrt{\frac{2\omega^2}{V\varepsilon_0}}\hat{p}(t)\cos(kz), \tag{3.10}$$

with the Hamiltonian in this form:

$$\hat{H} = \frac{1}{2}(\hat{p}^2 + \omega^2\hat{q}^2). \tag{3.11}$$

We saw that the electromagnetic field can be quantized by the association of a quantum-mechanical oscillator with each mode k of the radiation field. We can thus define new operators, called annihilation and creation operators, that aren't Hermitian but are more convenient:

$$\hat{a} = (2\hbar\omega)^{-1/2}(\omega\hat{q} + i\hat{p}) \tag{3.12}$$

$$\hat{a}^\dagger = (2\hbar\omega)^{-1/2}(\omega\hat{q} - i\hat{p}), \tag{3.13}$$

where $\hat{a}$ is the annihilation and $\hat{a}^\dagger$ is the creation operator. They satisfy the commutation relation: $[\hat{a}, \hat{a}^\dagger] = 1$. The operators $\hat{q}$; $\hat{p}$ can be written in terms of $\hat{a}$; $\hat{a}^\dagger$:

$$\hat{q} = \sqrt{\frac{\hbar}{2\omega}}(\hat{a} + \hat{a}^\dagger) \tag{3.14}$$

$$\hat{p} = -i\sqrt{\frac{\hbar\omega}{2}}(\hat{a} - \hat{a}^\dagger), \tag{3.15}$$

which means that the Hamiltonian can now take the form:

$$\hat{H} = \hbar\omega\left(\hat{a}^\dagger\hat{a} + \frac{1}{2}\right). \tag{3.16}$$

3.2 Quantum operators and states

If we want to correctly create and manipulate single or entangled photons we need to be able to find a probability that a given property of our field has a certain value. We also need to be able to calculate that value. In this chapter we present the quantum model required for single-mode field description in quantum optics and ways to calculate these values.

3.2.1 The number operator

The number operator $\hat{n}$ is defined as a product of $\hat{a}^\dagger$ and $\hat{a}$:

$$\hat{a}^\dagger \hat{a} = \hat{n}. \tag{3.17}$$

The Hilbert space for a single mode consist of all linear combination of number states: $|\Psi\rangle = \sum_{n=0}^{\infty} C_n |n\rangle$. This space has a special name: Fock space. The expectation value of $\hat{n}$ is the mean number of photons in certain modes.
Let $|n\rangle$ be an eigenstate of the single mode field (of the Hamiltonian operator (3.16)) with E_n as the eigenvalue:

$$\hat{H} |n\rangle = E_n |n\rangle , \tag{3.18}$$

and we say that $\hat{a}^\dagger$ pushes the energy eigenvalue E_n to a higher level $E_n + \hbar\omega$. It creates a quantum of energy, a photon. Similarly $\hat{a}$ destroys one quantum of energy and E_n is lowered to $E_n - \hbar\omega$. We denote the lowest energy level as E_0 with the corresponding eigenstate $|0\rangle$. Then:

$$\hat{a} |0\rangle = 0 \tag{3.19}$$

$$\hat{H} |0\rangle = \frac{1}{2}\hbar\omega |0\rangle , \tag{3.20}$$

so the lowest energy eigenvalue is equal to $\hbar\omega/2$. The energy eigenvalues, which can also be seen as the energy levels of quantum harmonic oscillator, are then:

$$E_n = \hbar\omega \left(n + \frac{1}{2} \right), \; n \in \mathbb{N}. \tag{3.21}$$

For the number operator can also write:

$$\hat{n} |n\rangle = n |n\rangle , \tag{3.22}$$

where $\langle n|n\rangle = 1$. If we let the annihilation and creation operator on $|n\rangle$, we get:

$$\hat{a} |n\rangle = \sqrt{n} |n-1\rangle \tag{3.23}$$

$$\hat{a}^\dagger |n\rangle = \sqrt{n+1} |n+1\rangle . \tag{3.24}$$

As we see the number state $|n\rangle$ can be generated from the vacuum state (or, as we called it, the lowest energy state) $|0\rangle$:

$$|n\rangle = \frac{(\hat{a}^\dagger)^n}{\sqrt{n!}} |0\rangle . \tag{3.25}$$

The discrete set of number states $\{|n\rangle\}_{n=0}^{\infty}$ is complete which means two properties:

$$\langle m|n\rangle = \delta_{mn} \tag{3.26}$$

$$\sum_{n=0}^{\infty} |n\rangle \langle n| = \mathbb{I} \tag{3.27}$$

Thanks to these two properties we can write $\forall |\psi\rangle \in \mathcal{H}$:

$$\sum_{n=0}^{\infty} \alpha_n |n\rangle , \tag{3.28}$$

where $\alpha_n = \langle n|\psi\rangle$, which is very convenient. The expectation value of the number operator, which gives the mean number of photons in the beam, is proportional to the intensity of the beam:

$$\langle \hat{n} \rangle = \langle \hat{a}^\dagger \hat{a} \rangle \propto \langle I \rangle . \tag{3.29}$$

This is going to be relevant for measuring the correlation function in section 7.2.2.

3.2.2 Quadrature operator

The quadrature operator is defined as follows:

$$\hat{x}_\lambda = \frac{1}{\sqrt{2}} \left[\hat{a} \exp(-i\lambda) + \hat{a}^\dagger \exp(i\lambda) \right] , \tag{3.30}$$

where λ is a real phase. Eigenstates $|x_\lambda\rangle$ of the quadrature operator, which are given by $\hat{x}_\lambda |x_\lambda\rangle = x_\lambda |x_\lambda\rangle$, are continuous, unlike those of the number operator, which are discrete:

$$\langle x_\lambda | x'_\lambda \rangle = \delta(x_\lambda - x'_\lambda) \tag{3.31}$$

$$\int_{-\infty}^{\infty} \mathrm{dx}_\lambda |x_\lambda\rangle \langle x_\lambda| = \mathbb{I}. \tag{3.32}$$

So for we can write $\forall |\psi\rangle \in \mathcal{H}$:

$$|\psi\rangle = \int \psi_\lambda(x) |x_\lambda\rangle \, \mathrm{dx}, \tag{3.33}$$

where $\psi_\lambda(x) = \langle x_\lambda|\psi\rangle$ provided that the integral is defined. If we take a normalized pure state $|\psi\rangle = \sum_{n=0}^{\infty} c_n |n\rangle$ then the overlap between $|\psi\rangle$ and x_λ is equivalent to a position representation of the states of the harmonic oscillator for $\lambda = 0$. It is equivalent to a momentum representation for $\lambda = \pi/2$.

3.2.3 Coherent states

If we were to ask which states remind us the most of the classical states it would be the coherent states $|\alpha\rangle$ that describe excitation of a single-mode field. Coherent state can be written using the number states:

$$|\alpha\rangle = \sum_{n=0}^{\infty} \exp(\frac{|\alpha|^2}{2}) \frac{\alpha^n}{\sqrt{n!}} |n\rangle , \tag{3.34}$$

where $\alpha \in \mathbb{C}$ correspond to the complex amplitude of our wave. The single-mode coherent states are generated by an operator called displacement operator $\hat{D}(\alpha)$ acting on the vacuum state. The displacement operator is unitary and can be defined as follows:

$$\hat{D}(\alpha) = \exp(\alpha \hat{a}^\dagger - \alpha^\star \hat{a}). \tag{3.35}$$

The coherent state can be written using the displacement operator:

$$|\alpha\rangle = \hat{D}(\alpha)\,|0\rangle\,, \tag{3.36}$$

from which we can derive the equation (3.34). Coherent states are normalized, meaning $\langle\alpha|\alpha\rangle = \mathbb{I}$, but they are not orthogonal. Their significance is nonetheless given by the fact that they are a right eigenstates of $\hat{a}$ with eigenvalue α:

$$\hat{a}\,|\alpha\rangle = \alpha\,|\alpha\rangle\,. \tag{3.37}$$

Because $\hat{a}$ and $\hat{a}^\dagger$ don't commute, $|\alpha\rangle$ is not a right eigenstate of $\hat{a}^\dagger$. However, $|\alpha\rangle$ is a left eigenstate of $\hat{a}^\dagger$ with eigenvalue $\alpha^\star$:

$$\langle\alpha|\,\hat{a}^\dagger = \alpha^\star\,\langle\alpha|\,. \tag{3.38}$$

The probability of finding n photons is given by:

$$p(n) = |\,\langle n|\alpha\rangle\,|^2 = \exp(-|\alpha|^2)\frac{\alpha^{2n}}{n!}, \tag{3.39}$$

which is a Poisson distribution. Coherent states ar fairly important as the laser radiation is a good approximation of them.

3.3 Multi-mode case

Results from section 3.1 can be generalized for multi-mode field. Again we assume electromagnetic fields in free space without sources of radiation and with no charges. Let's also assume the free space to be in shape of a cubic cavity of side length L with perfectly reflecting walls, $L >>$ atom sizes inside the cavity. We then impose periodic boundary conditions, for example in the x axis:

$$\exp(ik_x x) = \exp(ik_x + L), \tag{3.40}$$

from which we get:

$$k_x = \left(\frac{2\pi}{L}\right) m_x,\ m_x \in \mathbb{Z}. \tag{3.41}$$

Similarly for the y axis and the z axis:

$$k_y = \left(\frac{2\pi}{L}\right) m_y,\ m_y \in \mathbb{Z} \tag{3.42}$$

$$k_z = \left(\frac{2\pi}{L}\right) m_z,\ m_z \in \mathbb{Z} \tag{3.43}$$

from which we deduce the wave vector:

$$\vec{k} = \frac{2\pi}{L}(m_x, m_y, m_z). \tag{3.44}$$

The frequency is then given as follows:

$$\omega_k = |\vec{k}|c, \tag{3.45}$$

where c is the speed of light in vacuum. We now calculate the total number of modes, starting with the discrete case. The total number of modes in the intervals Δm_x, Δm_y and Δm_z is given by:

$$\Delta m_x \Delta m_y \Delta m_z = 2\left(\frac{L}{2\pi}\right)^3 \Delta k_x \Delta k_y \Delta k_z, \tag{3.46}$$

where the factor 2 corresponds to two polarization directions. If we assume wavelength much smaller than L, we get the quasi-continuum limit of equation (3.46):

$$\mathrm{dm} = 2\left(\frac{V}{8\pi^3}\right) \mathrm{dk_x dk_y dk_z}, \tag{3.47}$$

where $V = L^3$. We switch to spherical polar coordinates

$$\vec{k} = |\vec{k}|(\sin\theta\cos\phi, \sin\theta\sin\phi, \cos\phi) \tag{3.48}$$

which gives us:

$$\mathrm{dm} = 2\left(\frac{V}{8\pi^3}\right) k^2 \mathrm{dk d\Omega}, \tag{3.49}$$

where $\mathrm{d\Omega} = \sin\theta \mathrm{d}\theta \mathrm{d}\phi$. By using the dispersion relation (3.45), we get equation (3.49) in following form:

$$\mathrm{dm} = 2\left(\frac{V}{8\pi^3}\right) \frac{\omega^2 k}{c^3} \mathrm{d\omega_k d\Omega}. \tag{3.50}$$

We now integrate equation (3.50) over $\mathrm{d\Omega}$ which gives us the total number of modes in all directions in the range from ω_k to $\omega_k + \mathrm{d\omega_k}$:

$$N(\omega_k, \omega_k + \mathrm{d\omega_k}) = V\frac{\omega_k^2}{\pi^2 c^3} \mathrm{d\omega_k}. \tag{3.51}$$

Once we have determined the total number of all modes in our system, we can present the quantization. In analogy with the single-mode case and equation (3.11) we get the Hamiltonian of our system in a following manner:

$$H = \frac{1}{2}\sum_{\vec{k},s} (p_{\vec{k}s}^2 + \omega_k^2 q_{\vec{k}s}^2), \tag{3.52}$$

where $\vec{k}$ represents the set of integers (m_x, m_y, m_z) and s is a subscript for two orthogonal polarization directions.

3.3.1 Operators and states of multi-mode field

Annihilation and creation operators are given as follows:

$$\hat{a}_{\vec{k}s} = (2\hbar\omega_k)^{-1/2}\left(\omega_k \hat{q}_{\vec{k}s} + i\hat{p}_{\vec{k}s}\right), \tag{3.53}$$

$$\hat{a}_{\vec{k}s}^\dagger = (2\hbar\omega_k)^{-1/2}\left(\omega_k \hat{q}_{\vec{k}s} - i\hat{p}_{\vec{k}s}\right). \tag{3.54}$$

We can now quantize the Hamiltonian in analogy with (3.16):

$$\hat{H} = \sum_{\vec{k},s} \hbar\omega_k \left(\hat{a}^\dagger_{\vec{k}s} \hat{a}_{\vec{k}s} + \frac{1}{2} \right) = \sum_{\vec{k},s} \hbar\omega_k \left(\hat{n}_{\vec{k}s} + \frac{1}{2} \right). \tag{3.55}$$

As we can see, the number operator for the mode $\vec{k}s$ is given as $\hat{n}_{\vec{k}s} = \hat{a}^\dagger_{\vec{k}s} \hat{a}_{\vec{k}s}$. Each of these modes has a set of number eigenstates $|n_{\vec{k}s}\rangle$. We shall define the jth mode $\hat{n}_{\vec{k}_j s_j} \equiv \hat{n}_j$ to simplify the notation. The multi-mode photon state is then defined as a product of number states of all the modes:

$$|n_1\rangle |n_2\rangle |n_3\rangle ... \equiv |n_1, n_2, n_3, ...\rangle = |\{n_j\}\rangle , \tag{3.56}$$

which is an eigenstate of $\hat{H}$. Annihilation and creation operator of the jth mode are acting on the multi-mode state as:

$$\hat{a}_j |n_1, n_2, ...n_j, ...\rangle = \sqrt{n_j} |n_1, n_2, ...n_j - 1, ...\rangle \tag{3.57}$$

$$\hat{a}^\dagger_j |n_1, n_2, ...n_j, ...\rangle = \sqrt{n_j + 1} |n_1, n_2, ...n_j + 1, ...\rangle . \tag{3.58}$$

Number states can be generated from the vacuum state $|\{0\}\rangle = |0_1, 0_2, ...0_j, ...\rangle$ as follows:

$$|\{n_j\}\rangle = \prod_j \frac{\left(\hat{a}^\dagger_j\right)^{n_j}}{\sqrt{n_j!}} |\{0\}\rangle . \tag{3.59}$$

3.4 Non-linear quantum optics

The origin of non-linearity is described by the $\chi^{(n)}$ coefficients. If we want to calculate them we need to use time-dependent perturbation theory, which is incredibly complex and mathematically hard to solve. We can still go through the main thoughts of solving this problem, though. First we need to write down the Schrödinger equation:

$$\frac{\partial |\psi\rangle}{\partial t} = -\frac{i}{\hbar} \hat{H} |\psi\rangle , \tag{3.60}$$

where $\hat{H} = \hat{H}_0 + \hat{V}$ corresponds to unperturbed Hamiltonian $\hat{H}_0$ and a perturbation Hamiltonian $\hat{V} = -\hat{\vec{\mu}}\vec{E}$, where $\hat{\vec{\mu}}$ is the dipole operator. As we already know we can expand $|\psi\rangle$ in terms of energy eigenstates and we shall do so in two ways:

$$|\psi\rangle = \sum_n a_n |n\rangle = \sum_n b_n |n_t\rangle , \tag{3.61}$$

where $|n_t\rangle = |n\rangle \exp(-i\omega_n t) = |n\rangle \exp(\frac{-iE_n t}{\hbar})$, E_n represents the energy eigenvalue. Exact time dependence is hidden in a_n as

$$a_n = b_n \exp(-i\omega_n t), \quad \sum_n |a_n|^2 = \sum_n |b_n|^2 = 1. \tag{3.62}$$

If we put (3.61) to (3.60) we can then express the time evolution of our system in terms of a_n or b_n:

$$\dot{a}_n = -i\omega_n a_n - \frac{i}{\hbar} \sum_k V_{nk} a_k, \quad \dot{b}_n = -\frac{i}{\hbar} \sum_k V'_{nk} b_k, \tag{3.63}$$

where $V_{nk} = \langle n|\hat{V}|k\rangle$ is called the perturbation matrix element, $V'_{nk} = V_{nk}\exp(i\omega_{nk}t)$ and $\omega_{nk} = \omega_n - \omega_l$. If we were to calculate the expectation value of the dipole operator $\hat{\vec{\mu}}$ we could use coefficients a_n and b_n in equation (3.62):

$$\langle\hat{\vec{\mu}}\rangle = \langle\psi|\hat{\vec{\mu}}|\psi\rangle = \sum_{nk} a_k a_n^* \langle k|\hat{\vec{\mu}}|n\rangle = \sum_{nk} a_k a_n^* \vec{\mu}_{nk} = \sum_{nk} b_k b_n^* \langle k|\hat{\vec{\mu}}|n\rangle \exp(-i\omega_{nk}t) \quad (3.64)$$

The polarization vector is then given by:

$$\vec{P} = N\langle\hat{\vec{\mu}}\rangle = N\sum_{nk}\vec{\mu}_{nk}a_k a_n^*, \quad (3.65)$$

where N is the total atomic number density. The dipole operator $\hat{\vec{\mu}}$ can be written in matrix form:

$$\begin{pmatrix} 0 & \vec{\mu}_{01} \\ \vec{\mu}_{10} & 0 \end{pmatrix} \quad (3.66)$$

which will shortly be very convenient for us.
In the perturbation theory we expand the solution, in our case the probability amplitudes a_n, b_n and then an approximation is made by ignoring higher orders of $|\vec{\mu}|$:

$$a_n = a_n^{(0)} + a_n^{(1)} + a_n^{(2)} + a_n^{(3)} + ..., \quad (3.67)$$

where respective orders are implicitly hidden inside the coefficients. In our case there is no need to focus on orders higher that two or three. If we take the zeroth-order solution as $a_0^{(0)} = 1$ and $a_1^{(0)} = 1$, then equation (3.63) reads:

$$\dot{a}_1^{(1)} + i\omega_{10}a_1^{(1)} = -\frac{i}{\hbar}V_{10}, \quad (3.68)$$

where V_{10} is given by:

$$V_{10} = -\frac{1}{2}\sum_k \mu_{10}^k(\hat{E}_k\exp(i\omega t) + const.), \quad (3.69)$$

where the notation μ_{10}^k represents the k-th Cartesian component of $\vec{\mu}_{10}$. Equation (3.68) is then integrated, which gives us:

$$a_1^{(1)} = \frac{1}{2\hbar}\sum_k \mu_{10}^k\left(\frac{\hat{E}_k\exp(i\omega t)}{\omega_{10}+\omega} + \frac{\hat{E}_k^*\exp(-i\omega t)}{\omega_{10}-\omega}\right). \quad (3.70)$$

Now that we have the first-order component we can use it to derive the polarization of our medium:

$$P_i = N(a_0 a_1^*\mu_{10}^i + a_1 a_0^*\mu_{01}^i) \quad (3.71)$$

The linear susceptibility is then given by:

$$\hat{P}_i = \varepsilon_0\sum_k \chi_{ik}^{(1)}\hat{E}_k, \quad (3.72)$$

which means we get:

$$\chi_{ik}^{(1)} = \frac{N}{\varepsilon_0\hbar}\left(\frac{\mu_{01}^j\mu_{10}^i}{\omega_{10}^*-\omega} + \frac{\mu_{01}^j\mu_{10}^i}{\omega_{10}^*+\omega}\right). \quad (3.73)$$

As for the second order, we get by analogy:

$$a_2^{(1)} = \frac{1}{2\hbar}\sum_k \mu_{20}^k \left(\frac{\hat{E}_k \exp(i\omega t)}{\omega_{20}+\omega} + \frac{\hat{E}_k^* \exp(-i\omega t)}{\omega_{20}-\omega} \right) \tag{3.74}$$

and the second-order corrections can be derived from:

$$\dot{a_1^{(2)}} + i\omega_{10} a_1^{(2)} = -\frac{i}{\hbar} V_{12} a_1^{(2)} = \frac{i}{2\hbar}\sum_k \mu_{12}^k (\hat{E}_k \exp(i\omega t) + const.) a_2^{(1)}. \tag{3.75}$$

By putting (3.74) into (3.75) we get:

$$a_1^{(2)} = \frac{1}{4\hbar^2}\sum_{k,l} \mu_{12}^l \mu_{20}^k \left(\frac{\hat{E}_k \hat{E}_l \exp(2i\omega t)}{(\omega_{10}+2\omega)(\omega_{20}+\omega)} + \frac{\hat{E}_k^* \hat{E}_l^* \exp(-2i\omega t)}{(\omega_{10}-2\omega)(\omega_{20}-\omega)} \right). \tag{3.76}$$

By switching $1 \leftrightarrow 2$ we can get $a_2^{(2)}$. The final result for polarization of our media is then:

$$\begin{aligned} \hat{P}_i = \frac{N}{2\hbar^2}\sum_{k,l}\sum_{m,n} \Bigg(& \frac{\mu_{0m}^k \mu_{mn}^l \mu_{n0}^i}{(\omega_{m0}-\omega)(\omega_{n0}-2\omega)} + \frac{\mu_{0m}^l \mu_{mn}^i \mu_{n0}^k}{(\omega_{m0}-\omega)(\omega_{n0}+\omega)} \\ & + \frac{\mu_{0m}^i \mu_{mn}^k \mu_{n0}^l}{(\omega_{m0}+2\omega)(\omega_{n0}+\omega)} \Bigg) \hat{E}_k^\omega \hat{E}_l^\omega, \end{aligned} \tag{3.77}$$

where we put $(m,n) = (1,2)$ and then $(m,n) = (2,1)$.

Chapter 4

Quantum entanglement

In this thesis we covered two possible descriptions of light behaviour, the classical and the quantum. In dealing with the quantum world we often come across many strange concepts. We shall cover those in this section.

4.1 Polarization entanglement

A state of entangled photons is impossible to write down using just tensor product of two separate states:

$$|\psi\rangle \neq |H\rangle_A |V\rangle_B \tag{4.1}$$

where H, V describes polarization states (H for horizontal and V for vertical) and A, B describe spatial modes, but equation (4.1) applies for any quantum states of said photons. This means it is impossible to write the state of just one photon without mentioning the other. Our description must therefore have following form:

$$|\psi\rangle = |H\rangle_A |H\rangle_B \pm |V\rangle_A |V\rangle_B , \tag{4.2}$$

The biggest challenge in facing the entanglement, described in the next section 4.2, is that measuring the state of one particle affects the other one, no matter the distance between them, which is called non-locality. The idea of non-local effects involving entangled particles was first brought up by Einstein, Podolsky and Rosen in [8]. Details are discussed in the section below, 4.2.

4.2 Einstein-Podolsky-Rosen paradox

The idea of entanglement led to a very famous gedanken experiment that led to the EPR paradox. It went like this. Consider two particles from the same source travelling in opposite direction with their transverse position always correlated. We can write this state (called $|EPR\rangle$) down in position basis:

$$|EPR\rangle = \int \mathrm{dx} \, |x\rangle_A |x\rangle_B , \tag{4.3}$$

where $|x\rangle_i$ is a position eigenstate of the i-th particle. If we were to measure one of the particles position, then the position of the second particle would be the same, as with polarization states in previous section. Let's write the state (4.3) in momentum basis:

$$|EPR\rangle = \int \mathrm{dp}\, |p\rangle_A \langle p|_A \int \mathrm{dp}'\, |p'\rangle_B \langle p'|_B \int \mathrm{dx}\, |x\rangle_A |x\rangle_B = \tag{4.4}$$

$$= \int \mathrm{dp}\, |p\rangle_A \int \mathrm{dp}'\, |p'\rangle_B \int \mathrm{dx} \exp\left[\frac{i}{\hbar}(p+p')x\right] = \tag{4.5}$$

$$= \int \mathrm{dp}\, |p\rangle_A |-p\rangle_B\,, \tag{4.6}$$

where $|p\rangle_k$ represents momentum eigenstate of the k-th particle. Let's assume, that every object in our universe can only be influenced in accordance with laws of relativity a.k.a. it can not be influenced by objects outside its light cone. Let's also assume that the state of our particle exists prior to our measurements. Those two assumptions are called local realism. Now the problem is that if an observer chose to measure either position or momentum of the particle A, at the same time either position or momentum of the particle B would be also known to the observer. And if that observer was to measure either momentum or position, respectively, of the particle B, he would have a complete knowledge of both position and momentum of the particle B, which violates the Heisenberg principle. EPR assumed, that this is a proof of incompleteness of quantum theory and hence there must be additional variables, hidden to us, that determined the real situation. They came with the idea of class of theories called hidden variable theories, that should have replaced quantum description. For a long time there was no possibility to test whether quantum mechanics or hidden variable theories were more accurate. That was until a theoretician called J.S.Bell came with a way to experimentally test the difference, see [9]. Further information and mathematical apparatus behind EPR paradox can be found for example in [10].

4.3 Bell inequality

In 1965 Bell came up with a way to quantify the difference between quantum mechanics and hidden variable theories. It is an inequality that must be obeyed by all local realistic theories but could be violated by entangled systems as they exhibit quantum correlation, which should not be possible to achieve under classical physics. Let us have a same set-up as in previous section. Source emitting correlated beams with particles travelling opposite directions, A and B. They have two options for travelling, two possible paths. Since the easiest way to conduct this experiment in the laboratory is to work with entangled photons, as they are easily prepared nowadays, these two possible paths could represent two orthogonal polarization of photons, H and V.[1] There are few possibilities how to prepare an entangled photon pair, which will be covered in section 5.2. Now the two path available are combined and then spatially separated to form a different pair of orthogonal

[1]Since we work with polarization entanglement it should be noted that a much mathematically easier version of Bell inequality was developed by John Clauser, Michael Horne, Abner Shimony and Richard Holt, CHSH inequality for short. See more in [11].

paths, let's call them + and −. The combining is done in a way that it should be impossible to determine from + and − if a particle was H or V. We shall label this operation $C(\theta)$, where θ is a mixing parameter and it is some combination of polarization tools changing the original basis. Once a measurement is done on either + or − we get $R^{+}(\theta)$ or $R^{-}(\theta)$ as a result, respectively. A correlation function can be constructed as follows:

$$R^{ij}(\theta_A, \theta_B) = R^{i}_{A}(\theta_A) R^{j}_{B}(\theta_B), \tag{4.7}$$

where $i, j = +, -$. Let's now form the normalized averages, that also have the form of probabilities:

$$P^{ij}(\theta_A, \theta_B) = \frac{\langle R^{ij}(\theta_A, \theta_B)\rangle}{\sum_{k,l=\pm} \langle R^{kl}(\theta_A, \theta_B)\rangle}. \tag{4.8}$$

Correlations in any local realistic theory must then be bound by following inequality:

$$S = |E(\theta_A, \theta_B) + E(\theta'_A, \theta'_B) + E(\theta'_A, \theta_B) - E(\theta_A, \theta'_B)| \leq 2, \tag{4.9}$$

where

$$E(\theta_A, \theta_B) = P^{++}(\theta_A, \theta_B) + P^{--}(\theta_A, \theta_B) - P^{+-}(\theta_A, \theta_B) - P^{-+}(\theta_A, \theta_B). \tag{4.10}$$

Dealing with entangled states means equation (4.9) no longer holds for some choices of parameters θ_i, θ'_i, where $i \in \{A, B\}$. The maximum violation of the Bell inequality (which means maximal entanglement) happens for so called Bell states:

$$|\Phi^{\pm}\rangle = (|V\rangle_A |V\rangle_B \pm |H\rangle_A |H\rangle_B) \tag{4.11}$$

$$|\Psi^{\pm}\rangle = (|V\rangle_A |H\rangle_B \pm |H\rangle_A |V\rangle_B). \tag{4.12}$$

Chapter 5

Single-photon source

In this chapter we describe how single polarized photon behaves, how to prepare such quantum state and how to create entangled photon pair in the laboratory. Sources of information for this chapter were mainly [6] and [12].

5.1 Polarization of single photon

To assign a horizontal or vertical polarization state to a photon is not such a problem. The confusion starts once we try to combine polarization planes in the same manner we do in classical optics. Let us first define what does a polarization of a single photon mean. Suppose we have a horizontal/vertical polarizing beam splitter. If a photon exits through the horizontal port, we define it as being in state $|H\rangle$. Similarly if a photon exits through a vertical port, we assign it a vertical state $|V\rangle$. So far so good. Interesting things start happening once we switch to a diagonal/anti-diagonal photons as its state suddenly changes to either $|H\rangle$ or $|V\rangle$ from the original state. In classical optics half of the beam that is polarized either diagonally or anti-diagonally goes through one port, while the other half goes through the second port. If we send a photon in state $|D\rangle$ or $|A\rangle$ through the beam splitter it is then absolutely unpredictable which port it chooses (a.k.a. what new state is changes to). All that is known to us is that half of the photons goes through one port and the other half goes through the second port. If we were to describe this we would start with following assumptions:

$$\langle H|V\rangle = \langle V|H\rangle = 0 \tag{5.1}$$

$$\langle H|H\rangle = \langle V|V\rangle = 1. \tag{5.2}$$

The states $|D\rangle$ and $|A\rangle$ can be written in terms of $|V\rangle$ and $|A\rangle$ which can be done as follows:

$$\langle D|A\rangle = \langle A|D\rangle = 0 \tag{5.3}$$

$$\langle D|D\rangle = \langle A|A\rangle = 1 \tag{5.4}$$

$$|D\rangle = \frac{1}{\sqrt{2}}(|H\rangle + |V\rangle) \tag{5.5}$$

$$|A\rangle = \frac{1}{\sqrt{2}}(|H\rangle - |V\rangle). \tag{5.6}$$

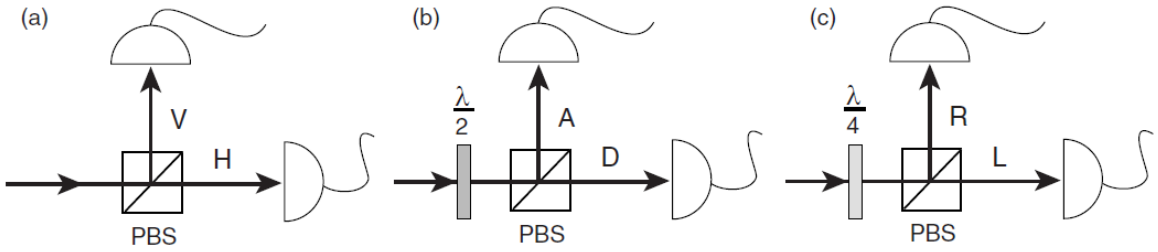

Figure 5.1: Preparation of different polarization states. $\lambda/2$ refers to a half-wave plate, $\lambda/4$ refers to a quarter-wave plate. Ad a) horizontal/vertical polarization, ad b) diagonal/anti-diagonal polarization, ad c) left/right circular polarization. The optical axes of half-wave plate and quarter-wave plate are rotated 45° with respect to the optical axis of PBS. Source [13].

We can also define the right circular photon polarization state $|R\rangle$ and the left circular polarization state $|L\rangle$ in the same manner:

$$\langle R|L\rangle = \langle L|R\rangle = 0 \tag{5.7}$$

$$\langle R|R\rangle = \langle L|L\rangle = 1 \tag{5.8}$$

$$|R\rangle = \frac{1}{\sqrt{2}}(|H\rangle + i\,|V\rangle) \tag{5.9}$$

$$|L\rangle = \frac{1}{\sqrt{2}}(|H\rangle - i\,|V\rangle). \tag{5.10}$$

Definition of all the states are depicted in figure 5.1. As a conclusion, any polarization state can be written as follows:

$$|\psi\rangle = a\,|H\rangle + \exp(i\phi)b\,|V\rangle\,, \tag{5.11}$$

where $a^2 + b^2 = 1$ and $a, b, \phi \in \mathbb{R}$.

5.2 Spontaneous parametric down-conversion source

Spontaneous parametric down-conversion (SPDC) is a non-linear optical process during which a photon from a laser (called pump) is converted into two photons (signal and idler) under energy and momentum conservation. Those two emerging photons are entangled. The crystal needs to posses a $\chi^{(2)}$ non-linearity, which in this case is a tensor of rank 3. The polarization vector is the given by:

$$P_i = \varepsilon_0 \sum_{j,k=1,2,3} \chi_{ijk} E_j E_k, \tag{5.12}$$

where $i \in \{1, 2, 3\}$ and E_j, E_k are terms of the electro-magnetic field in (1.2). There are three types of SPDC processes. Type-0 couples pump, signal and idler with the same polarization. In type-I the pump polarization plane is orthogonal to the signal and idler. Lastly, in type-II SPDC process, the signal and idler are orthogonally polarized. The

classical approach can however not fully explain the PDC process, which is the reason why we shall switch to the quantum approach. The SPDC Hamiltonian is described as follows:

$$\hat{H}^{PDC} \propto \chi^{(2)} \int_{-\frac{L}{2}}^{\frac{L}{2}} \hat{E}_p^{(+)}(z,t)\hat{E}_s^{(-)}(z,t)\hat{E}_i^{(-)}(z,t)\mathrm{dz}, \tag{5.13}$$

where p, s, i labels pump, signal and idler field respectively and the operators $\hat{E}$ are defined as:

$$\hat{E}_x^{(+)} = \hat{E}_x^{(-)\dagger} = const. \int \exp[i(k_x(\omega_x)z - \omega_x t)]\hat{a}_x(\omega_x)\mathrm{d}\omega_\mathrm{x}, \tag{5.14}$$

where $k(\omega_x)$ is a propagation constant and $\hat{a}_x(\omega_x)$ is the annihilation operator for a monochromatic frequency. Substituting equation (5.14) into (5.13) gives us en expression proportional to $\hat{a}^\dagger\hat{a}^\dagger\hat{a}$ and $\hat{a}^\dagger\hat{a}\hat{a}$ which corresponds to one photon decaying in two daughter photons and vice versa. Parametric down-conversion source produces good optical modes with good spacial characteristics and strongly correlated photons. If one daughter photon is detected in one arm, any other photon detected in the other arm of the set-up in any short time interval will be its twin. So any information about one of the photons from the emerging pair can be used to condition the other. This makes the PDC source a good approximation to a single-photon source.

5.2.1 Waveguided crystal PDC

The waveguide technology lies in confinement of signal and idler fields over large distances which enables production of pure single photons with high brightness. They also enable coupling to optical fibres and integration into optical circuits, which makes them very practical. Waveguides operate under a single mode regime and only for specific wavelengths which needs to be taken into consideration. The waveguides used in our experiments (see section 7.2) are in-house fabricated by metal-diffusion (rubidium exchanged waveguides) in potassium titanyl phosphate ($KTiOPO_4$). They are made to be most efficient for wavelengths around $\lambda_p \simeq$ 700nm. The PDC process in waveguides happens under certain circumstances, mainly under conservation of energy and momentum:

$$\omega_p = \omega_s + \omega_i \tag{5.15}$$

$$\vec{k_p} = \vec{k_s} + \vec{k_i}, \tag{5.16}$$

where the subscripts p, s, i correspond to pump, signal and idler respectively. Our PDC source produces single photons under type-II SPDC so it is possible to separate them by a polarizing beam splitter afterwards. This separation makes it easier to distinguish between them which is making any experimental implementation much practical.

Chapter 6

Single-photon detection techniques

In this chapter we shall explore possible ways of detecting single photons or an entangled pair. We will elaborate on various ways of light detection in the laboratory and give a brief overview of the most important characteristics that evaluate detector performance.

6.1 Photodetectors

Our aim is to explore properties of PDC sources and create entangled photon pairs. As we already discussed earlier, proper understanding of the physics behind photon counting and single-photon manipulation will inherently lead to construction of functioning quantum computational devices and further exploration of quantum cryptography. Detection of light in this cases happen through conversion to electric signal which is then analysed. We can either detect bright fields, which is basically intensity measurements, or weak fields, which correspond to photon number counting. Most widely used detectors for such single-photon counting measurements are those semiconductor-based, mainly photodiodes. In our experimental set-ups for entangled photons detection two free-space coupled single-photon counting modules were used, see section 7.1. We shall now briefly discuss their principle of operation.
There are three possible ways of detection in photon counters: photochemical, photoelectric and photo thermal. In the photochemical case the incoming photon triggers a chemical change that can later be detected. In the photo thermal case the photon is converted to a phonon, which then creates a temperature change. We use the photoelectric way of detection where the incoming photon is converted to an electron. Fast electric signal can be provided either by Photo-Multiplier Tube or by Avalanche photodiode (APD).

6.1.1 Avalanche photodiodes

APD makes use of the photovoltaic effect in a semiconductor crystal. A photodiode can be described as a p-n diode operated in reverse bias, once the incoming photon with energy $E_\gamma = h\nu$ hits the detector it is absorbed and an electron hole pair is created. This process depends on the incoming photon wavelength as well as on conversion efficiency, which can

be described as follows:

$$\eta_{conv} = \frac{h\nu}{q}\frac{I}{P_{in}}, \tag{6.1}$$

where I [A] is the generated current given by applied electric field, mobility of electric charge carriers as well as by cross-section of the active area of our detector. Once the photon energy $E_\gamma = h\nu$ is acquired by an electron, it is no longer trapped in valence band and moves to the conduction band. This mechanism is illustrated in Fig. (6.1). Once an external voltage is applied, electrons are able to flow very quickly and the conversion efficiency η_{conv} is increased. These moving electrons than manage to cause secondary ionization which then leads to an avalanche breakdown in the crystal. This mode of operation is also called the Geiger mode. The p-n junction is then switched to the ON state with a constant macroscopic current flow. Avalanche is then quenched and the voltage can be reset. Each avalanche breakdown produces a large electrical pulse and

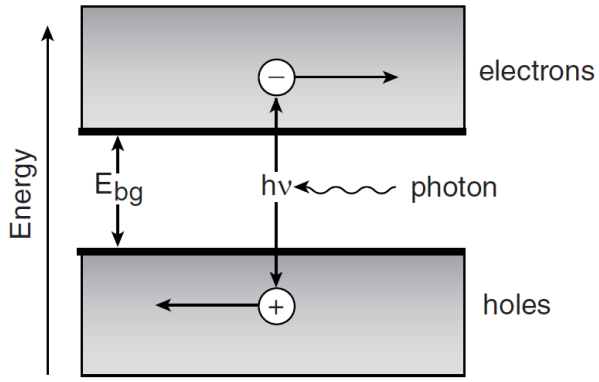

Figure 6.1: Illustration of a band gap in APD. APDs are often run in Geiger mode to amplify the signal to measurable value. Source: [13].

corresponds to a detection of a single photon. We call this breakdown a click. Thanks to a very short response time (in nanoseconds) and low voltage supply, photodiodes are very often used for coincidence measurements. Another thing that makes them very efficient is the output which is digitalized and is usually in the form of TTL pulses.

6.1.2 Superconducting nano-wire detector

Another detector was also used for our data evaluation, which was a superconducting nano-wire single-photon detector (SNSPD) from a company called Photon spot. They are the fastest single-photon counters in the world currently available. The detection part consists of a nano-wire (under 10 nm thin and 200 nm wide) with a pixel at its end, which is cooled below its superconducting critical temperature, usually around 10° K, which means that electrons inside form Cooper pairs[1]. Once a photon hits the nano-wire it breaks a pair, which results in electrical resistance larger than 50 ohm and generates a measurable electric pulse. The wire then cools down and becomes sensitive to incoming

[1]Cooper pair can be described as a pair of fermions in a state with energy lower than the Fermi energy, which then makes the two fermions bound. This pair state is then responsible for superconductivity.

photons with reset time in nanoseconds. In order to make the incident photon hit the active area, an optical fibre must be brought very close and aligned properly. There is also a different absorption efficiency for different polarization direction. Photons polarized in the direction of the nano-wire are absorbed better. For this reason we have fibre polarization controllers added so we are actually able to change the polarization plane of the incident photons. SNSPD is much faster than APD, has lower background noise and shorter dead time (in orders of nanoseconds). It has detection efficiency larger than 85% for certain wavelengths (in comparison APD has detection efficiency around 20%). All these important characteristics of single-photon counters are discussed in details in the section below.

6.1.3 Photodetector characteristics

First very important characteristic is the **quantum efficiency**, η_Q, which represents the probability of incoming photons being converted to electric signal. This parameter depends on the material used and on the spectral response of the detector, meaning that every detector has a maximum quantum efficiency for different wavelengths. If we were to calculate the overall efficiency of a free space coupled detector, we must also take into account the absorption efficiency, η_{abs}, which tells us what portion of incoming photons was absorbed in the photosensitive material of the detector, plus the threshold efficiency, η_{thr}, which tells us if the electric signal created was registered by our electronic devices. The overall detection efficiency can be described as follows:

$$\eta_{det} = \eta_Q \eta_{abs} \eta_{thr}. \tag{6.2}$$

Another very important characteristic of a photodetector is the **dark noise**, sometimes called dark count rate. There is always some signal detected even when the light source is blocked. Main reasons behind such events are mostly material impurities and thermal effects. The higher detection precision, the better, so there is always an effort to bring the dark noise to the lowest level possible, which is usually achieved by cooling. The semiconductor photodiode temperature in our experiments is usually as low as $-50°$C.
The **background noise**, also called background count rate, must also be taken into account. This property is not the detector's fault, some detectors can be more susceptible to this type of noise though, mainly the ones most sensitive to far-infrared radiation.
The next characteristic we will talk about is the detector sensitivity, which can be defined as the minimum power detectable P_{in} [W], and responsivity, which responds to the amount of current generated with incoming P_{in}. This characteristic differs from efficiency, which is independent from wavelength. Responsivity varies with incident energy.
Some other important parameters include response times, namely **dead time**, which corresponds to the duration of time during which a detection system is incapable of producing an output electrical signal. The detection efficiency η_{det} during the dead time is close to zero.
Lastly we shall talk about the **active area** of the detector, which is the area that absorbs incoming photons. Being able to couple the device correctly mostly means making the portion of incoming signal hitting the active area as large as possible. Our previous set-

up, see section 7.1, was defective mostly because of non-sufficient coupling to the counting modules active area, which is the reason why we didn't have enough counts and weren't able to finish the measurements.

6.2 Coincidence counting

Detecting coincidence means correctly evaluating discrete events, especially the time and place of particle arrival. The photons arrive under some distribution, like Poissonian, if the light source is a laser (hence produces coherent states, see section 3.2.3) or regularly spaced in time, if they come from a single photon source (that produces Fock states, see section 3.2.1). Two or more detectors need to be connected to a coincidence counter in order to correctly evaluate all the data and eliminate as much noise as possible. Such noise usually comes from dark counts and background. The coincidence counter only sends a signal once both detectors send pulses in a time window T, which is as narrow as possible. T can also be called resolution time. A pulse comes from either detector at time $t^{(1)}+T_t^{(1)}$, where $T_t^{(1)}$ is a transit time from the detector to the coincidence counter. In order for the counter to send a signal, following condition must be met:

$$|(t^{(2)} + T_t^{(2)}) - (t^{(1)} + T_t^{(1)})| < T. \tag{6.3}$$

The reason why coincidence counting is so important is a low probability of a false signal. Let's label the probability of a background single-photon detection p_i, where i represents individual detectors. By the laws of conjoint probability, the possibility of a coincidental background detection is then $p_1 p_2$, where in fact $p_1 = p_2$, since both detectors preceding coincidence unit are usually the same and have the same characteristics, so the overall probability is p_1^2. Hence a chance false signal is detected drops by a power of two. The overall theory behind coincidence counting in quantum optics is robust and complicated. In our experimental set-up for entangled pair production and detection (see section 7.1) a coincidence unit was made out of integrated circuits. Theory and details of construction are given in my Bachelor's thesis [14].

Chapter 7

Conducted experiments

7.1 Entangled-photons experiment

Our aim in this experiment was to create and detect quantum entangled photon pairs. The process of construction and calibration of our old set-up is presented in detail in my Bachelor's thesis [14]. The source we used was a BBO crystal that produced single-photons under the first type of SPDC, which means that the photons were polarized in the same plane. Sadly we weren't able to detect enough photons so we decided to consult our experiment with the Integrated Quantum Optics group in Paderborn university. We decided to change our previous set-up to a new one, see figure 7.1. This new set-up has not been tested yet as we plan to construct it in new laboratory that is under construction. The laser beam goes first through a wave-plate to change the polarization plane of the

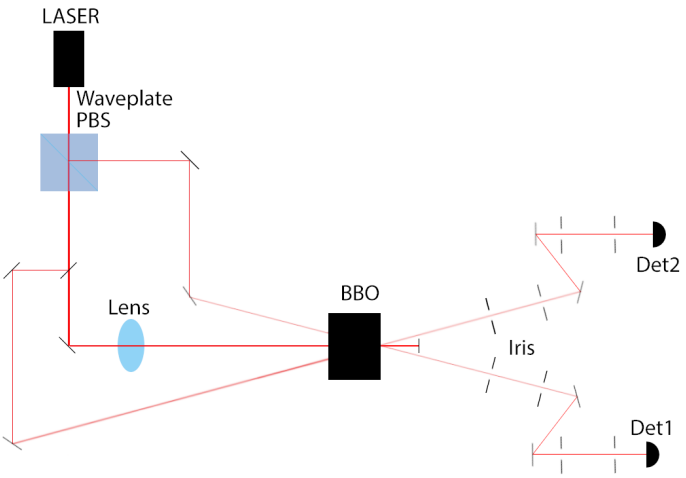

Figure 7.1: A new set-up for entangled photon pairs.

pump. Then it travels to a polarizing beam splitter (PBS) mainly for coupling purposes. As we see in figure 7.1 two different beams emerge from PBS and a third one is separated by a mirror. The two beams, narrower in the picture, are polarized in the same plane as signal and idler photons emerging from BBO are. This should allow us to couple the beam correctly to BBO and then to the detectors. The thick beam, which is going through the centre of PBS, is the pump which then travels to a lens that focuses is to BBO. As we

already mentioned, this set-up has not been tested yet so further adjustments might be needed.

7.2 IQO Paderborn experiments

Few experiments were carried out in collaboration with Integrated Quantum Optics group in Paderborn university, Germany. We were provided with a PDC source in form of a 16 mm long KTP crystal, which was manufactured in Paderborn laboratory. The waveguided KTP was designed to be spatially single-mode which helps to confine the field in a very small area for a very long propagation length. Several measurements were performed on this crystal in order to properly test its properties: coincidence measurements (correlations between the signal and idler photons produced), Klyshko efficiency and measurements of the second order correlation function. Corresponding experimental set-up is shown together with key components in figure 7.2. The beam source is a titanium-sapphire laser

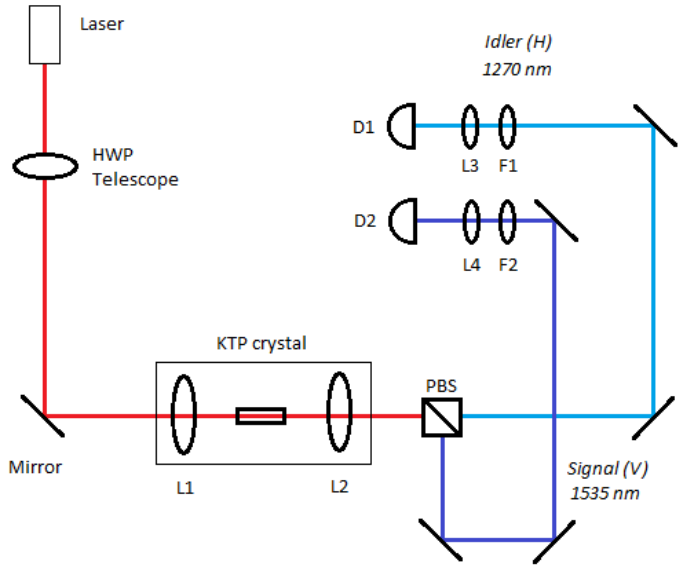

Figure 7.2: Experimental alignment for waveguide characterisation. Titanium-sapphire laser (laser), half-wave plate (HWP), fixed magnification beam expander GBE02-B from Thorlabs (telescope), C240 TME-B lens from Thorlabs (L1), C240 TME-B lens from Thorlabs (L2), KTP crystal (KTP), polarizing beam splitter (PBS), two hard coated edgepass filters from Thorlabs (F1, F2) blocking $\lambda_p = 695\,\text{nm}$, two A397TM-C lenses from Thorlabs (L3, L4), detectors (D1, D2).

with 300 fs long pulses with 12.5 ns between each of them. Wavelength of the beam is $\lambda_p = 670\,\text{nm}$, where the subscript p corresponds to pump. Light then goes through a half-wave plate to switch the polarization plane from vertical to horizontal. Then the beam travels through a telescope which then focuses it to one spot. It is then coupled to a waveguide in the KTP crystal through a lens (L1). KTP works as a single-photon source and also as entangled photon pair source, see more in section 5.2, so after travelling through the crystal both the single and the idler photon γ_s, γ_i emerge with wavelengths

$\lambda_i = 1270\,\text{nm}$ and $\lambda_s = 1535\,\text{nm}$, which is in the near-infrared telecommunication regime. They travel to a polarizing beam splitter which splits their paths. The two paths that the γ_s and γ_i can take are marked by dark or light blue colour. After that they are detected by either detector 1 or 2.

7.2.1 Klyshko efficiency

Klyshko developed an efficient method for single photon counter calibration as non-classical states change their statistics upon experiencing loss. Photons from PDC source emerge always in pairs which means they are correlated in photon number. So if we have a click in one arm we know for sure that there was a photon lost in the second arm. The efficiency is given for both signal and idler arm by:

$$\eta_i = \frac{cc}{c_s} \tag{7.1}$$

$$\eta_s = \frac{cc}{c_i}, \tag{7.2}$$

where cc denotes coincidence counts and c_i, c_s mean counts in signal and idler path respectively. After substituting all values necessary we get:

$$\eta_i = \eta_{D1} = 17\%, \tag{7.3}$$

$$\eta_s = \eta_{D2} = 35\%. \tag{7.4}$$

There is one more thing that needs to be done while calculating the detection efficiency. SNSPD detectors (see section 6.1.2) are very sensitive to polarization planes of incident photons. Using the formula (6.2) we divide (7.3) by different factor, which is $0,6$ for the idler path and $0,9$ for signal path. This gives us quite better results:

$$\eta_i = \eta_{D1} = 28\%, \tag{7.5}$$

$$\eta_s = \eta_{D2} = 38\%. \tag{7.6}$$

7.2.2 Second order correlation function

The second order correlation function $g^{(2)}$ is used to quantify intensity fluctuations of an electromagnetic field. This gives us information about our light source e.g. photon statistics and the measurement will show directly if a field is a quantum field or a classical field. It is given by:

$$g^{(2)}(\tau) = \frac{\langle I(t)I(t+\tau)\rangle}{\langle I(t)\rangle^2}, \tag{7.7}$$

where intensity $I(t)$ gives us the beam intensity at time t. τ represents time interval after which intensity $I(t+\tau)$ is detected. Using τ instead of specific time dependence is a simplification that can be made once the statistical properties are stationary. Since number of counts detected by a photon counter is proportional to the intensity, we can write $g^{(2)}$ using number states (see section 3.2.1):

$$g^{(2)}(\tau) = \frac{\langle \hat{n}^2\rangle - \langle \hat{n}\rangle}{\langle \hat{n}\rangle^2}. \tag{7.8}$$

There are several different outcomes for $g^{(2)}$ measurements. If we had a coherent (single mode) field, then $g^{(2)}(0) = 1$. For a Fock state $g^{(2)}(0) = 1 - 1/n < 1$. To measure this function we split path of γ_s in two by a fibre beam-splitter which enabled us to measure coincidences between three detector instead of two. Corresponding set-up can be seen in figure 7.3. Several measurements were made with different source power. Since we were

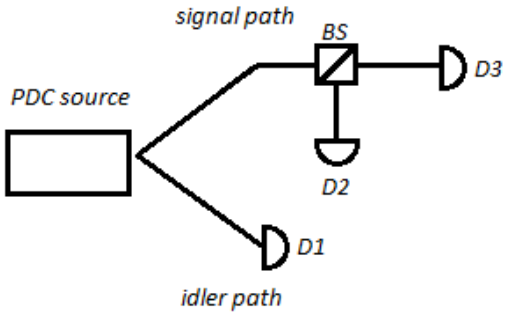

Figure 7.3: Experimental alignment for heralded single-photon preparation and $g^{(2)}$ evaluation. BS is fibre beam-splitter.

detecting clicks and coincidences, our $g^{(2)}$ function was evaluated as:

$$g^{(2)} = N\frac{ccc_{123}}{cc_{12}cc_{13}}, \tag{7.9}$$

where different subscripts correspond to different detectors, cc_{ij} represents number of coincidence counts between two detectors i, j and ccc_{ijk} represents number of coincidence counts between three detectors i, j, k. N is a normalizing factor which in our case is number of counts detected by detector 1. Final results after data evaluation can be seen in figure 7.4. The second order correlation function gives us different results for classical

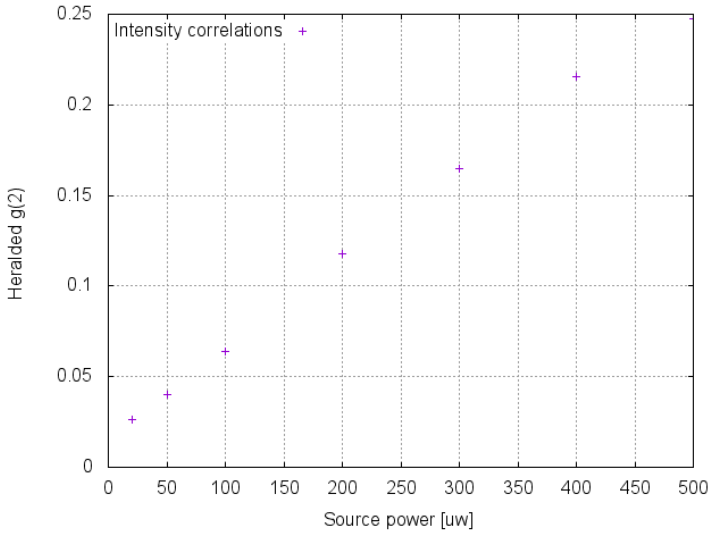

Figure 7.4: Heralded $g^{(2)}$ function for different source power.

and quantum light sources. For bunched light[1] it is always greater than one, $g^{(2)}(\tau) > 1$. For coherent (laser) light $g^{(2)}(\tau) = 1$ and for anti-bunched light $g^{(2)}(\tau) < 1$. As we see in figure 7.4, the values of $g^{(2)}$ are smaller and slowly approaching 1 for all intensities. This is an experimental proof that we actually produced single photons.

[1]Bunched and anti-bunched light are terms for classical and non-classical light. In classical cases the light arrives to detector in "bunch" that can be described by classical optics. On the other hand for non-classical light photons arrive at separate times and are more regularly spaced.

Conclusion

We provided the base for theoretical background necessary for understanding light propagation, field quantization and single-photon generation. We also described construction of several experimental set-ups and showed that we actually created and detected single photons. In the future we want to further increase the Klyshko efficiency and minimize the size of the integrated optical circuit. This includes not only better coupling, but also better source characterization and more efficient detection. In case of better coupling we plan to run a simulation to calculate the most efficient wave propagation through out optical elements and to also create correct spatial modes, which are necessary in order to efficient propagation through optical wires. We also want to focus on better mounts for the KTP crystal, again in order to increase the coupling efficiency.

Bibliography

[1] Robert W Boyd. *Nonlinear optics*. Elsevier, 2003.

[2] Geoffrey New. *Introduction to nonlinear optics*. Cambridge University Press, 2011.

[3] Eugene Hecht. *Optics, 4th. edition*. International edition, Addison-Wesley, San Francisco, 2002.

[4] Frank L Pedrotti, Leno M Pedrotti, and Leno S Pedrotti. *Introduction to optics*. Cambridge University Press, 2017.

[5] Joseph W Goodman. *Introduction to Fourier optics*. Roberts and Company Publishers, 2005.

[6] Christopher Gerry, Peter Knight, and Peter L Knight. *Introductory quantum optics*. Cambridge university press, 2005.

[7] Stephen M Barnett and Paul M Radmore. *Methods in theoretical quantum optics*, volume 15. Oxford University Press, 2002.

[8] Albert Einstein, Boris Podolsky, and Nathan Rosen. *Can quantum-mechanical description of physical reality be considered complete?* Physical review, 47(10):777, 1935.

[9] John Stuart Bell. *On the einstein-podolsky-rosen paradox*. Physics, 1: 195–200, 1964.

[10] John Garrison and Raymond Chiao. *Quantum optics*. Oxford University Press, 2008.

[11] John Clauser, Michael Horne, Abner Shimony, and Richard Holt. *Proposed experiment to test local hidden-variable theories*. Physical review, 23:880, 1969.

[12] Ariel Lipson, Stephen G Lipson, and Henry Lipson. *Optical physics*. Cambridge University Press, 2010.

[13] Hans-Albert Bachor and Timothy C Ralph. *A guide to experiments in quantum optics*. Wiley, 2004.

[14] Elisabeth Andriantsarazo. *Provázané fotony a jejich interakce s biologickými strukturami*. FJFI ČVUT, 2017.